Actin Modifies Ca^{2+} Block of Epithelial Na^+ Channels in Planar Lipid Bilayers

Bakhrom K. Berdiev,* Ramon Latorre,† Dale J. Benos,* and Iskander I. Ismailov*
*Department of Physiology and Biophysics, University of Alabama at Birmingham, Birmingham, Alabama 35294-0005 USA and
†Centro de Estudios Científicos, Valdivia, and Departamento de Biologia, Facultad de Ciencias, Universidad de Chile, Santiago, Chile

ABSTRACT The mechanism by which the cytoskeletal protein actin affects the conductance of amiloride-sensitive epithelial sodium channels (ENaC) was studied in planar lipid bilayers. In the presence of monomeric actin, we found a decrease in the single-channel conductance of α-ENaC that did not occur when the internal $[Ca^{2+}]_{free}$ was buffered to <10 nM. An analysis of single-channel kinetics demonstrated that Ca^{2+} induced the appearance of long-lived closed intervals separating bursts of channel activity, both in the presence and in the absence of actin. In the absence of actin, the duration of these bursts and the time spent by the channel in its open, but not in its short-lived closed state, were inversely proportional to $[Ca^{2+}]$. This, together with a lengthening of the interburst intervals, translated into a dose-dependent decrease in the single-channel open probability. In contrast, a $[Ca^{2+}]$-dependent decrease in α-ENaC conductance in the presence of actin was accompanied by lengthening of the burst intervals with no significant changes in the open or closed (both short- and long-lived) times. We conclude that Ca^{2+} acts as a "fast-to-intermediate" blocker when monomeric actin is present, producing a subsequent attenuation of the apparent unitary conductance of the channel.

INTRODUCTION

Cytoskeletal elements participate in many cellular events (Kabsch and Vandekerckhove, 1992; Mills and Mandel, 1994; Cowin and Burke, 1996; Zigmond, 1996; Janmey, 1998; Hu and Reichardt, 1999; Fuchs and Yang, 1999), including regulation of a variety of ion transport events (see Cantiello, 1995; Smith and Benos, 1996; Cantiello and Prat, 1996; Cantiello, 1997a,b; Hilgemann, 1997; Sheng and Pak, 2000 for reviews). Such a role for the cytoskeleton has been also proposed regarding regulation of epithelial amiloride-sensitive sodium channels (Smith et al., 1991; Cantiello et al., 1991; Prat et al., 1993; Staub et al., 1996). More recently, following the cloning of the three Epithelial Na^+ Channel (ENaC) (Canessa et al., 1993, 1994; Lingueglia et al., 1993) subunits, we used a planar lipid bilayer reconstitution technique to study ENaC-cytoskeleton interactions (Berdiev et al., 1996; Ismailov et al., 1997a). In this system, we found that actin induced a two-fold reduction of ENaC single-channel conductance accompanied by an increase in channel open probability (P_o). The present study was performed to investigate specifically the mechanism(s) underlying the effect of actin on ENaC conductance.

To simplify the interpretation of the data, we restricted our experiments to studying the effects of actin on single channels formed by α-ENaC alone. We found that the actin-induced reduction of the single-channel conductance was independent of the degree of actin polymerization, but was completely abolished by buffering $[Ca^{2+}]_{free}$ in the solution bathing the ENaC-containing bilayers to <10 nM. Elevation of $[Ca^{2+}]$ in the presence of actin resulted in a concentration-dependent decrease in α-ENaC unitary conductance, with no apparent changes in channel P_o. In contrast, raising $[Ca^{2+}]$ in the absence of actin led to a dose-dependent decrease in channel P_o, with no changes in conductance. Analyses of the kinetic properties of ENaCs revealed that, both in the presence and in the absence of actin, elevation of $[Ca^{2+}]$ induced the appearance of relatively long lived closed events separating bursts of ENaC activity. The Ca^{2+}- induced decrease in single-channel P_o in the absence of actin was referable to elongation of these interburst intervals, shortening of the time spent by ENaC in its open state, and a decrease in the mean burst time of ENaC. In the presence of actin, the duration of the interburst intervals and the mean open time of ENaC were virtually independent of $[Ca^{2+}]$, whereas the mean burst time of ENaC was inversely related to $[Ca^{2+}]$. These findings can be interpreted as arising from the effects of Ca^{2+} acting as a "slow-to-intermediate" blocker of the open channel in the absence of actin, and as a "fast" blocker in the presence of actin.

MATERIALS AND METHODS

Reagents and solutions

Actin, purified from rabbit muscle (a kind gift of Dr. Steven S. Rosenfeld, University of Alabama at Birmingham), was diluted to a final concentration of 10 mg/ml with a buffer containing (in mM): Tris, 2; $CaCl_2$, 0.2; MgATP, 0.2; and mercaptoethanol, 0.2, pH 8.0, and added to the bilayer chamber (of 4 ml in volume) to reach a final concentration of 2.4 μM. This addition of actin resulted in the introduction of 2.068 μM of MgATP and $CaCl_2$ into the bathing solution, which was taken into account when calculating final concentrations of free divalent cations using the Bound-

Dr. Ismailov's present address is Department of Neurobiology, University of Alabama at Birmingham, Birmingham, AL 35294 USA

Address reprint requests to Dale J. Benos, Ph.D., Dept. of Physiology and Biophysics, UAB, MCLM 704, 1530 3rd Ave. S, Birmingham AL 35294-0005. Tel.: 205-934-6220; Fax: 205-934-2377; E-mail: benos@physiology.uab.edu.

and-Determined program (Brooks and Storey, 1992). To ensure that actin remained in the monomeric form, all of our experiments studying effects of varying $[Ca^{2+}]$ on ENaC (including the control recordings in the absence of actin) were performed in the presence of 4 μM DNase in the bathing solution. Phospholipids were purchased from Avanti Polar Lipids (Alabaster, AL). All other chemicals were reagent grade, and all solutions were made with distilled water and filter sterilized before use (Sterivex-GS, 0.22 ìm filter, Millipore Corp., Bedford, MA).

In vitro translation of ENaC

α-rENaC protein (a kind gift of Dr. B. Rossier, Lausanne, Switzerland) was in vitro translated using a TnT T7 Quick Coupled Transcription/Translation System kit (Promega, Madison, WI) according to manufacturers instructions in the presence of canine microsomal membranes (Promega, Madison, WI) and 0.8 mCi/ml [^{35}S]Trans label (ICN, Costa Mesa, CA). A 25-μl translation reaction was mixed with 0.5 mg phosphatidylethanolamine, 0.3 mg phosphatidylserine, 0.2 mg phosphatidylcholine, and 25 μl of a buffer containing 60 mM tris-(hydroxymethyl)-aminomethane (Tris) pH 6.8, 0.4% Triton X-100 (v/v), and 25% glycerol (v/v). The translated proteins were eluted from a G-150 superfine Sephadex (Pharmacia Biotech., Inc.) gel filtration column (5 mm in diameter, 2 ml in volume) with a buffer containing 500 mM NaCl, 0.1 mM EDTA, and 10 mM Tris (pH 7.6), and Triton X-100 (0.2%, v/v). 100 μl fractions were collected, and counted to determine the fractions with highest level of [^{35}S] incorporation.

Reconstitution into proteoliposomes

Three 100-μl fractions displaying the highest level of [^{35}S] incorporation were mixed with a phospholipid mixture (phosphatidylethanolamine: phosphatidylserine:phosphatidylcholine at a ratio of 50:30:20 w/w). Final volume was brought up to 600 μl with 400 mM KCl buffer supplemented with 5 mM Tris/HCl, 0.5 mM $MgCl_2$, 50 μM DTT, pH 7.4. To remove Triton X-100, samples were mixed with 150-mg Bio-Beads SM-2 (Bio-Rad, Melville, NY) and rotated at room temperature for 45 min, followed by overnight incubation at 4°C. Proteoliposomes were separated from the beads using a 1-ml syringe, sonicated for 40–45 s at 43 kHz (160 Watts), and allowed to re-form by freeze-thawing three to five times. This procedure resulted in dissociation of putative individual conduction elements of ENaC held together by sulfhydryl bonds (Ismailov et al., 1996). After DTT-treatment, single amiloride-sensitive Na^+ selective channels with uniform conductance of 13 pS in more than 70% of total incorporations were observed (Berdiev et al., 1998, Ismailov et al., 1999). Divided into 25-μl aliquots, proteoliposomes were stored at −70°C. Mock controls were prepared by performing the in vitro translation reaction in the absence of ENaC cRNA, and reconstituting the purified reaction products into proteoliposomes following an identical protocol.

Planar lipid bilayer experiments

Proteoliposomes were fused with the Mueller–Rudin planar lipid bilayers made of a 2:1 (wt:wt) diphytanoyl-phosphatidyl-ethanolamine/diphytanoyl-phosphatidylserine solution in *n*-octane (final lipid concentration 25 mg/ml). The bilayers were bathed with symmetrical 100 mM NaCl, 10 mM Tris-MOPS buffer (pH 7.4), supplemented with 100 μM EGTA. Single-channel currents were measured using a conventional current-to-voltage converter with a 10-GΩ feedback resistor (Eltec, Daytona Beach, FL) as described previously (Ismailov et al., 1997b). The identity and orientation of ENaCs in the membrane was tested at the end of each experiment by adding 0.5 μM amiloride to the *trans* compartment of the bilayer chamber. Single-channel analyses were performed using pCLAMP 6.0 software (Axon Instruments, Burlingame, CA) on current records low-pass filtered at 300 Hz through an 8-pole Bessel filter (902 LPF, Frequency Devices, Haverhill, MA) before acquisition using a Digidata 1200 interface (Axon Instruments). The actual number of functional ENaC channels in each given experiment was determined by transiently activating them (including those initially "silent") by establishing a hydrostatic pressure gradient across the membrane (Awayda et al., 1995; Ismailov et al., 1996). Bilayers containing multiple channels were not used.

RESULTS

We first tested the hypothesis that the effects of actin on ENaC conductance were not associated with the elongation of actin filaments. This hypothesis was based on the following observations: 1) alterations in both the conductance and the P_o of ENaC were evident at concentrations of actin ($\geq$0.6 μM) and ionic conditions (100 mM NaCl, ~10 μM $[Ca^{2+}]_{free}$) under which spontaneous polymerization of this cytoskeletal protein occurs (Carlier et al., 1986a,b; Kinosian et al., 1991; Cooper et al., 1983). 2) changes in P_o, but not in ENaC conductance, displayed a characteristic time course that correlated with that expected for actin filament formation. Because divalent cations are required for the formation of actin filaments in solution (Pollard and Cooper, 1986), we first determined the effects of actin on α-ENaC when $[Ca^{2+}]_{free}$ in the bilayer bathing solution was buffered to <10 nM. Depletion of $[Ca^{2+}]_{free}$ in the solution increased the fraction of time ENaC remained open from 0.6 to 0.95 (compare first and second traces in Fig. 1 *A*). Subsequent addition of actin at concentrations up to 2.4 μM under these nominally Ca^{2+}-free conditions did not change ENaC conductance or kinetics (Fig. 1 *A*, *third trace*). To ensure that actin remained in its monomeric form, we used deoxyribonuclease I (DNase I), an endonuclease that forms a tight 1:1 association with G-actin (Mannherz et al., 1975), thus preventing its polymerization (Hitchcock et al., 1976; Hitchcock, 1980). Moreover, DNase I can cause depolymerization of any filamentous actin (Hitchcock et al., 1976; Hitchcock, 1980). Figure 1 *B* depicts representative current traces of α-ENaC in the presence of DNase I. No changes in channel activity were observed after addition of DNase I under nominally Ca^{2+}-free conditions (Fig. 1 *B*, *first* and *second traces*). Addition of up to 2.4 μM actin produced no changes in ENaC properties (*third trace*), unless $[Ca^{2+}]$ was in the micromolar range (*fourth trace*).

We next designed experiments to investigate the mechanism(s) underlying the effects of monomeric actin on channel conductance. We varied $[Ca^{2+}]_{free}$ in the α-ENaC bathing solution in the presence or in the absence of actin. If Ca^{2+} ions were essential for the effect(s) of actin on ENaCs, a dependence of channel conductance on $[Ca^{2+}]$ would be expected. Figures 2 and 3 illustrate the results of experiments testing this prediction. Increasing the Ca^{2+} concentration in the absence of actin produced relatively long channel closures, resulting in a dose-dependent (K_D = 20.2 ± 4.6 μM; N = 4) decrease in single-channel P_o (Fig. 2, *A* and *B*). Single-channel conductance remained unchanged (13 pS, Fig. 2 *C*). In contrast, raising $[Ca^{2+}]$ in the

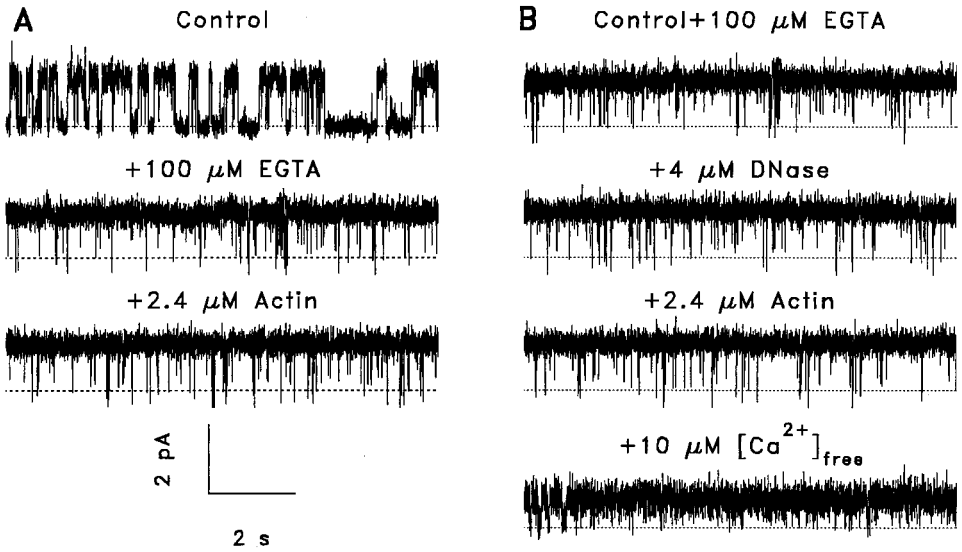

FIGURE 1 Effect of nonpolymerized actin on α-ENaC incorporated into planar lipid bilayer. Bilayers were bathed with symmetrical 100 mM NaCl, 10 mM MOPS-Tris (pH 7.4) solution containing 100 μM EGTA. Holding potential was +100 mV referred to the virtually grounded *trans* chamber. Records shown were filtered at 300 Hz with an 8-pole Bessel filter before acquisition at 1 ms per point using pCLAMP software (Axon Instruments). The level of free $[Ca^{2+}]$ was calculated using the Bound-and-Determined computer program (Brooks and Storey; 1992). Polymerization of actin (2.4 μM, added to the both compartments) was prevented by buffering $[Ca^{2+}]_{free}$ in (*A*) bilayer bathing solutions with 100 μM EGTA, or (*B*) by addition of 4 μM DNase I. Traces shown in (*A*) and (*B*) are representative of at least six and five experiments, respectively.

presence of actin caused no apparent change in P_o of the channel (Fig. 3, *A* and *B*), but resulted in a dose-dependent ($K_D = 5.8 \pm 1.9$ μM; $N = 5$) decrease in the single-channel conductance (Fig. 3, *A* and *C*).

Another potential contributor to the decrease in single-channel conductance of ENaC is Mg^{2+}, which was introduced into the bathing solution together with actin mostly in the form of Mg-ATP. If polymerization of actin occurred in the presence of DNase, hydrolysis of 2.068 μM of Mg-ATP (the maximal concentration that could be achieved at a final concentration of actin of 2.4 μM) could result in the release of an equivalent amount of Mg^{2+} (Pollard and Weeds, 1984; Korn et al., 1987; Carlier et al., 1987; Carlier et al., 1988; Carlier, 1990; Estes et al., 1992). In a solution buffered with 100 μM EGTA, 90–100% of this Mg^{2+} should exist as free ion (Brooks and Storey, 1992). However, in control experiments, the single-channel properties (P_o or conductance) of ENaC in the presence of 2 μM of Mg^{2+} in the bathing solution were statistically indistinguishable from those measured in the absence Mg^{2+}, either in the absence or presence of actin (data not shown). In addition, a gradual decrease in conductance was observed when free Ca^{2+} was elevated, in spite of the $[Mg^{2+}]_{free}$ remaining unchanged (Fabiato and Fabiato, 1979; Tsien, 1980; Bers, 1982; Smith and Miller, 1985; Harrison and Bers, 1989). Based on these findings, we conclude that the effect of actin on ENaC conductance can be attributed to monomeric (or G-) actin, and requires the presence of Ca^{2+} ions in the bathing solution.

Under nominally Ca^{2+} free conditions, in the absence or in the presence of monomeric actin (*upper panels* in Fig. 4, *A* and *B*, respectively), a single exponential function describes well both the closed and the open time distributions, with ~10 ms and 300–400 ms constants, respectively. Increasing $[Ca^{2+}]_{free}$ in the bathing solutions caused a decrease in the duration of time spent by the channel in its open state (in the absence, but not in the presence of actin) and the appearance of a second, relatively long-lived closed state (τ_c''), with no change in the time spent by the channel in its initial short-lived closed state (τ_c') (both in the absence and in the presence of actin, see Fig. 4, *A* and *B*). Table 1 depicts statistically treated numerical data for the open and closed time constants determined for each experimental condition.

DISCUSSION

A parsimonious interpretation of these findings is that the changes in channel behavior observed both in the presence and in the absence of monomeric actin could arise from a block of ENaC by Ca^{2+}. Consider the blocking scheme,

$$\text{Closed} \underset{\alpha}{\overset{\beta}{\rightleftarrows}} \text{Open} \underset{k_{off}}{\overset{k_{on}[\text{Blocker}]}{\rightleftharpoons}} \text{Blocked}.$$

SCHEME 1

This model predicts that the reciprocal mean open time ($1/\tau_o$) is given by the relation,

$$1/\tau_o = \alpha + k_{on}[\text{Blocker}], \quad (1)$$

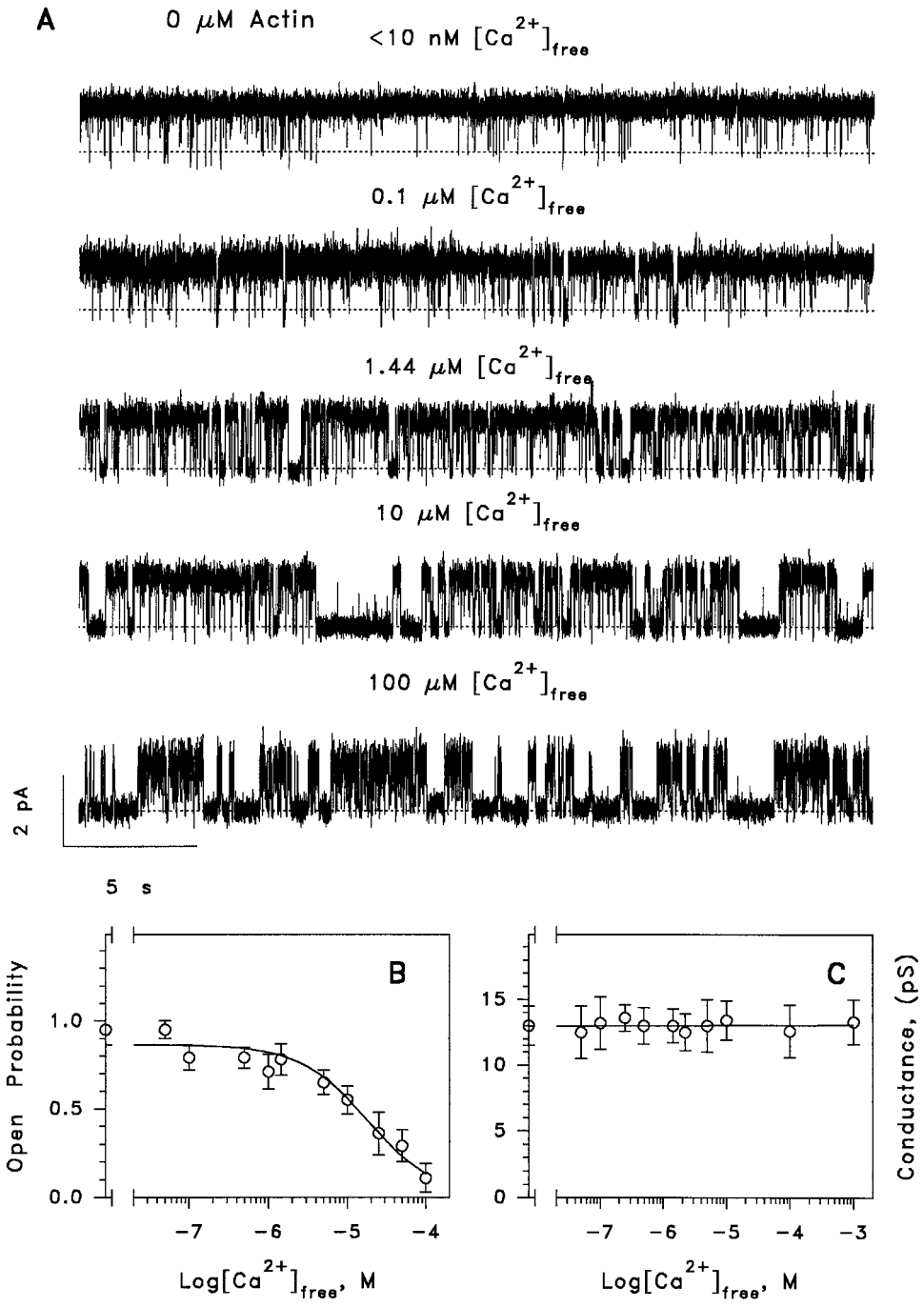

FIGURE 2 Effect of Ca^{2+} on α-ENaC in planar lipid bilayers in the absence of actin. (*A*) Recording and acquisition conditions were the same as for Fig. 1. To ensure that actin remained in the monomeric form, all of our experiments studying effects of varying $[Ca^{2+}]$ on ENaC (including the control recordings in the absence of actin) were performed in the presence of 4 μM DNase in the bathing solution. The final free Ca^{2+} concentrations indicated above the traces, were calculated using the Bound-and-Determined computer program. Additions of EGTA (100 μM) and Ca^{2+} were made to both compartments of the chamber. Traces shown are representative of at least six experiments. (*B*) $[Ca^{2+}]$-dependence of α-ENaC open probability in the absence of actin. Line in the plot represents a fit of the data to the first-order Michaelis–Menten equation $P_o = P_{omax}(1 - [Ca^{2+}]/(K_D + [Ca^{2+}]))$ (Eq. 8) with a K_D of $18.2 \cdot 10^{-6}$ M. (*C*) Summary plot of single-channel unitary conductance of α-ENaC as a function of $[Ca^{2+}]$. Line in the plot is a linear regression fit of the data.

and the 1/mean blocked time ($1/\tau_{blocked}$) as

$$1/\tau_{blocked} = k_{off}. \quad (2)$$

In agreement with the predictions of kinetic Scheme 1, the reciprocal plots of ENaC lifetimes as a function of $[Ca^{2+}]$ showed that the mean channel open time was indeed inversely proportional to $[Ca^{2+}]$ in the absence of actin (Fig. 5*A*). In the presence of actin, however, this parameter was independent of $[Ca^{2+}]$ (Fig. 5 *D*).

Understanding the nature of the two closed states of ENaC observed in the presence of Ca^{2+} both in the presence and in the absence of actin is complex because of the difficulty in distinguishing between the times spent by a channel in a closed versus a blocked state. The basic kinetic Scheme 1 predicts that the blocked time (which is the inverse of k_{off}) should be independent of the blocker concentration. In our analyses, this was true for the short-lived closed time, both in the presence or in the absence of actin

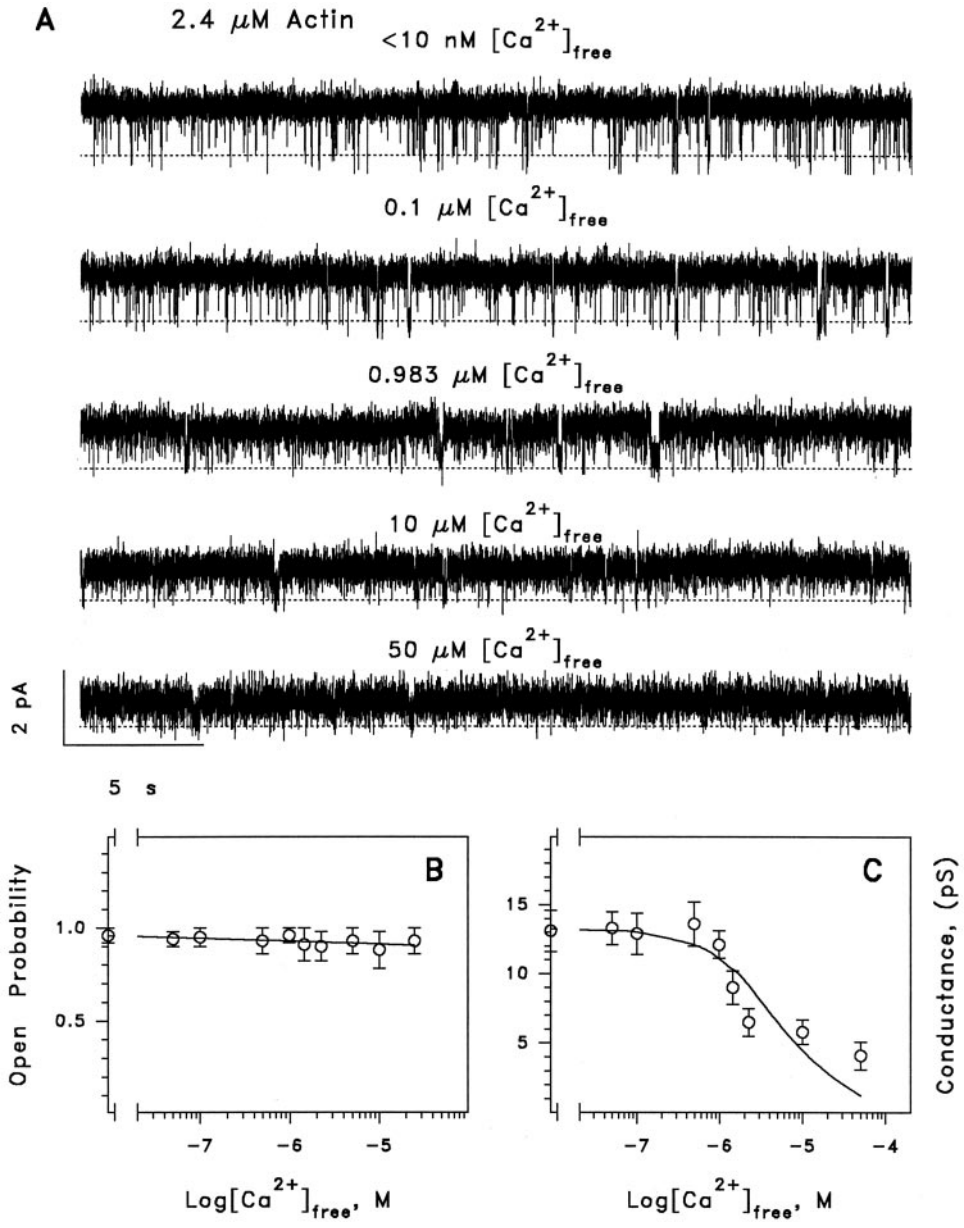

FIGURE 3 Effect of Ca^{2+} on α-ENaC in planar lipid bilayers in the presence of globular actin. (*A*) Recording conditions were the same as for Fig. 1. Actin (2.4 μM), EGTA (100 μM), 4 μM DNase, and Ca^{2+} (shown above the traces) were present in both compartments of the chamber. Traces shown are representative of at least 5 experiments. (*B*) Summary plot of α-ENaC open probability as a function of $[Ca^{2+}]$. Line in the plot is a linear regression fit of the data. (*C*) $[Ca^{2+}]$-dependence of single-channel unitary conductance of α-ENaC in the presence of actin. Line in the plot represents a fit of the data to the first-order Michaelis–Menten equation $g = g_{max}(1 - [Ca^{2+}]/(K_D + [Ca^{2+}]))$ (Eq. 9) with a K_D of $5.1 \cdot 10^{-6}$ M.

(see Fig. 5, *B* and *E*). However, short closures with a similar mean closed time were also present in the nominal absence of Ca^{2+}. If the blocking reaction is slower than the gating reaction, the appearance of the periods of fast channel gating (bursts) flanked by slow closures would be expected. The kinetic pattern of ENaC in the presence (but not in the absence) of Ca^{2+} resembles this description. If the second, long-lived, closed state of ENaC induced by Ca^{2+} were the periods when the channel was blocked, their duration should be independent of the blocker concentration. The plot of the reciprocal mean time spent by the channel in the long-lived closed state in the presence of actin, complied with this prediction (Fig. 5 *F*). In the absence of actin, however, the mean time of the channel residing in this state was a linear function of $[Ca^{2+}]$ (Fig. 5 *C*). This result suggests the presence of several blocked states in series,

$$\text{Open} \rightleftarrows \text{Blocked}_1 \rightleftarrows \text{Blocked}_2 \rightleftarrows \cdots \rightleftarrows \text{Blocked}_i,$$

SCHEME 2

where the probability of finding the channel in a given blocked state is dependent on the concentration of $[Ca^{2+}]$. Recall that the duration of the short (~10-ms) closures of ENaC were independent of $[Ca^{2+}]$ and were present even in the nominal absence of Ca^{2+}. Moreover, their frequency increased as $[Ca^{2+}]$ was elevated. This is possible if the rate constant for entering the blocked state is similar to that of

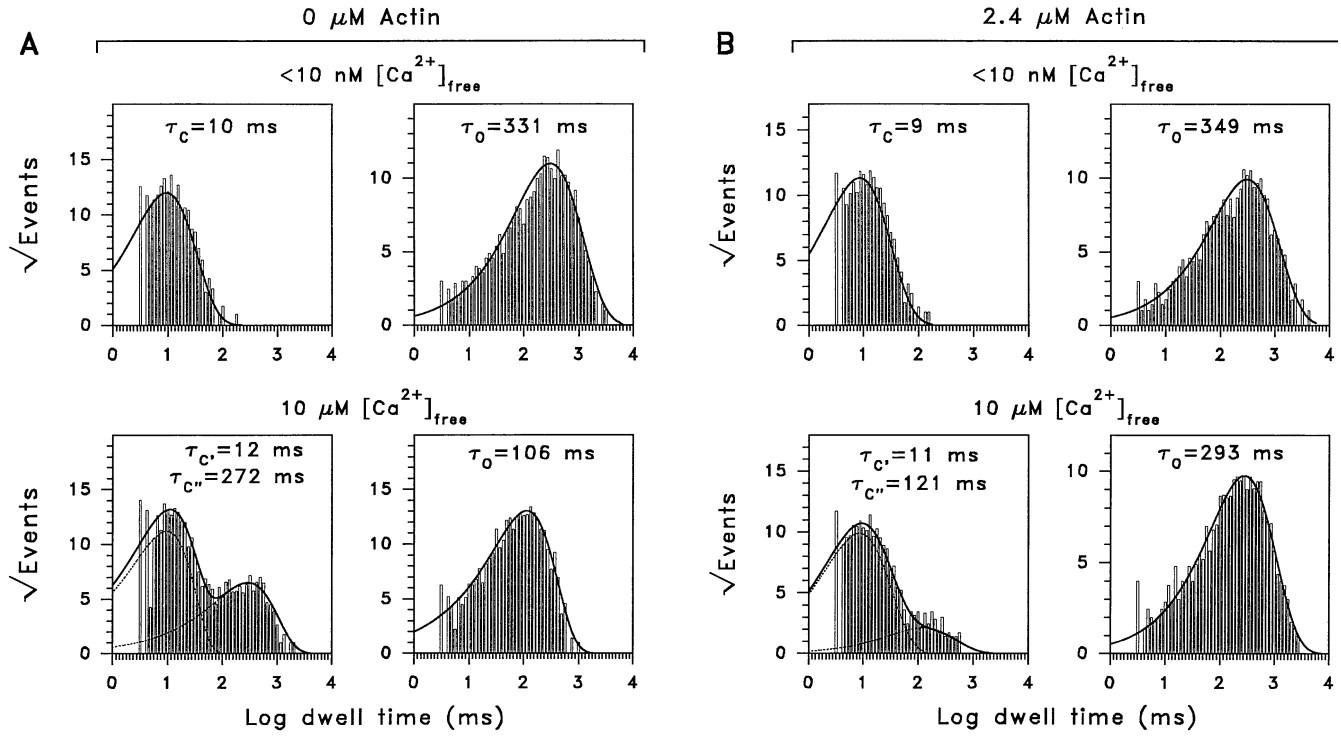

FIGURE 4 Effect of $[Ca^{2+}]$ on kinetic properties of α-rENaC in planar lipid bilayers in the absence and in the presence of actin. Representative dwell-time histograms were constructed following the events analyses performed using pCLAMP software (Axon Instruments) on single-channel recordings of 10 min in duration filtered and acquired as described in Fig. 1. The event detection thresholds were 50% in amplitude of transition between closed and open states, and 3 ms in duration. Closed and open time constants shown were determined by fitting the closed and open time histograms to the probability density function $g(x) = \Sigma_{j=1}^{k} a_j g_o(x - s_j)$ (Eq. 10), where s_j is the logarithm of the jth time constant, and a_j is the fraction of total events represented by the jth component (Sigworth and Sine, 1987), and using the Simplex least square routine of pSTAT. The number of bins per decade in all histograms was 16. Numbers of events used for construction of the closed and open time histograms shown were: 2249 and 2248 (0 μM Actin; <10 nM Ca^{2+}), 3638 and 3637 (0 μM Actin; 10 μM Ca^{2+}), 1866 and 1867 (2.4 μM Actin; <10 nM Ca^{2+}), 1798 and 1797 (2.4 μM Actin; 10 μM Ca^{2+}), respectively.

the gating process itself,

$$\text{Closed} \underset{\alpha}{\overset{\beta}{\rightleftarrows}} \text{Open} \underset{k_{\text{off fast}}}{\overset{k_{\text{on fast}}[Ca^{2+}]}{\rightleftarrows}} \text{Blocked}_{\text{fast}} \underset{k_{\text{off slow}}}{\overset{k_{\text{on slow}}}{\rightleftarrows}} \text{Blocked}_{\text{slow}},$$

SCHEME 3

where $k_{\text{on fast}} \approx \alpha$. In this case, the number of fast blocked events per unit open time N_B, is

$$N_B = k_{\text{on fast}}[Ca^{2+}]P_o, \quad (3)$$

where the P_o is the conditional probability of the channel being open, given that it can reside in one of the two states, open and closed. This conditional open probability is effectively the open probability inside a burst. The experimental values for these parameters at each given $[Ca^{2+}]$ can be calculated as follows. The number of the fast blocked events is assumed to be the total number of events spent by the channel in the short-lived closed state (*dotted lines* in the representative closed time histograms in Fig. 4, *A* and *B*). The total time spent by the channel in the open state is given by the integral of the probability density function fitting the open time histogram. The open probability inside the burst can be calculated as a ratio of the total time spent by the channel in the open state to the total time spent by the channel in the short-lived closed state (calculated as the integral of the probability density function fitting the short-lived component of the closed-time histogram). These analyses demonstrate that, in the absence of actin, the frequency of the appearance of the fast closed state of ENaC is a linear function of $[Ca^{2+}]$ with a slope of $4.7 \cdot 10^5$ $M^{-1}s^{-1}$ (Fig. 5 *G*), which is in good agreement with the $k_{on} = 5.1 \cdot 10^5$ $M^{-1}s^{-1}$ calculated as the slope of the $1/\tau_o$ versus $[Ca^{2+}]$ plot. In the presence of actin, however, the slope of the plot of the frequency of the fast closed state of ENaC was $1.6 \cdot 10^4$ $M^{-1}s^{-1}$. Thus, we conclude that, at least in the absence of actin, it is purely coincidental that there is an absence of a second fast closed state corresponding to the Ca^{2+} block. Although the experimental data show only two well-defined closed states, it is possible that other blocked states are actually present at different $[Ca^{2+}]$.

If the long quiescent periods that were virtually absent in the absence of Ca^{2+} do correspond to $\text{Blocked}_{\text{slow}}$ in Scheme 3, some predictions for the duration of bursts of channel activity can be made. The termination of a burst in

TABLE 1 Effect of $[Ca^{2+}]_{free}$ on kinetic properties of α-ENaC in bilayers in the absence and in the presence of actin

$[Ca^{2+}]_{free}$ (μM)	State: Open τ_o (M ± m, ms)	State: Closed, short-lived τ'_c (M ± m, ms)	State: Closed Long-lived τ''_c (M ± m, ms)	Minimum total number of single channel events fitted in a single experiment	Number of experiments
0 μM Actin					
<0.01	343 ± 31	9 ± 5	—	3305	13
0.01	293 ± 38	10 ± 7	90 ± 24	3225	9
0.1	315 ± 33	9 ± 4	100 ± 27	3266	9
0.491	264 ± 34	10 ± 5	111 ± 29	3873	8
0.983	231 ± 29	9 ± 5	106 ± 32	4083	7
1.44	222 ± 43	10 ± 5	114 ± 41	5012	5
5	132 ± 31	12 ± 6	136 ± 39	5579	4
10	109 ± 27	10 ± 5	220 ± 38	6488	6
25	66 ± 21	11 ± 6	310 ± 49	6528	7
50	34 ± 13	10 ± 4	909 ± 161	9497	6
100	16 ± 8	9 ± 5	4203 ± 647	6785	4
2.4 μM Actin					
<0.01	338 ± 35	10 ± 6	—	3351	17
0.01	336 ± 42	9 ± 7	—	3403	12
0.1	284 ± 34	10 ± 5	95 ± 12	3612	11
0.491	298 ± 41	11 ± 6	99 ± 16	3421	5
0.983	328 ± 34	10 ± 7	104 ± 13	3181	7
1.44	293 ± 45	9 ± 6	104 ± 18	3229	6
5	295 ± 40	10 ± 5	94 ± 13	3413	6
10	318 ± 37	11 ± 4	102 ± 17	3087	7
25	294 ± 44	10 ± 5	90 ± 19	3524	4
50	307 ± 34	11 ± 4	108 ± 21	3514	5

this case is exiting the set of closed, open, and fast blocked states, and the rate constant for this transition is the inverse of the mean burst duration (τ_{burst}) times a conditional probability of being in a burst (P_{burst}),

$$k_{on\ slow} = (1/\tau_{burst}) \cdot P_{burst}, \quad (4)$$

where

$$P_{burst} = P_{blocked\ fast} = \frac{k_{on\ fast}[Ca^{2+}]}{k_{on\ fast}[Ca^{2+}] + k_{off\ fast}}. \quad (5)$$

The analyses of burst kinetics of ENaC as a function of $[Ca^{2+}]$ are shown in Fig. 6. The distributions of burst times of ENaC activity at different $[Ca^{2+}]_{free}$ in the absence and in the presence of actin can be fit to a single exponential (Fig. 6, *A* and *B*, respectively). Table 2 shows statistically treated numerical data for duration of bursts at different $[Ca^{2+}]$. The plot of the reciprocal dwell-time constants obtained from these fits as a function of $[Ca^{2+}]$ is shown in Fig. 6 *C*. In the absence of actin, $1/\tau_{burst}$ tends to saturate, just as predicted from Eqs. 4 and 5. In the presence of actin, increasing $[Ca^{2+}]_{free}$ resulted in an elongation of these burst periods. This result is possible if the rate of blocking/unblocking transition is fast compared to the closing reaction (both modified by actin). Burst termination occurs because the channel enters the closed state,

$$\text{Closed}' \underset{\alpha'}{\overset{\beta'}{\rightleftarrows}} \text{Open}' \underset{k'_{off\ fast} \gg \beta'}{\overset{k'_{on\ fast}[Ca^{2+}] \gg \alpha'}{\rightleftharpoons}} \text{Blocked}'_{fast}.$$

SCHEME 4

The mean burst time is given by,

$$\tau_{burst} = 1/\alpha' \cdot P'_{burst}, \quad (6)$$

where

$$P'_{burst} = P'_o = \frac{k'_{off\ fast}}{k'_{on\ fast}[Ca^{2+}] + k'_{off\ fast}}. \quad (7)$$

Therefore, τ_{burst} will increase linearly with $[Ca^{2+}]$. Thus, in the absence of actin, Ca^{2+} acts as a slow-to-intermediate blocker of an open ENaC; in the presence of actin, this block becomes fast. If the time scale of "flickering" exceeds the limit of resolution of the recording system, the unitary conductance of the channel appears to be lowered (Vergara and Latorre, 1984; Yellen, 1984; Villarroel et al., 1988; Green et al., 1987; Wang, 1988).

To conclude, we have found that the reduction of the single-channel conductance of ENaC in the presence of actin is independent of polymerization of this cytoskeletal protein, but depends on the presence and concentration of Ca^{2+} ions in the bathing solution. The results of analyses of

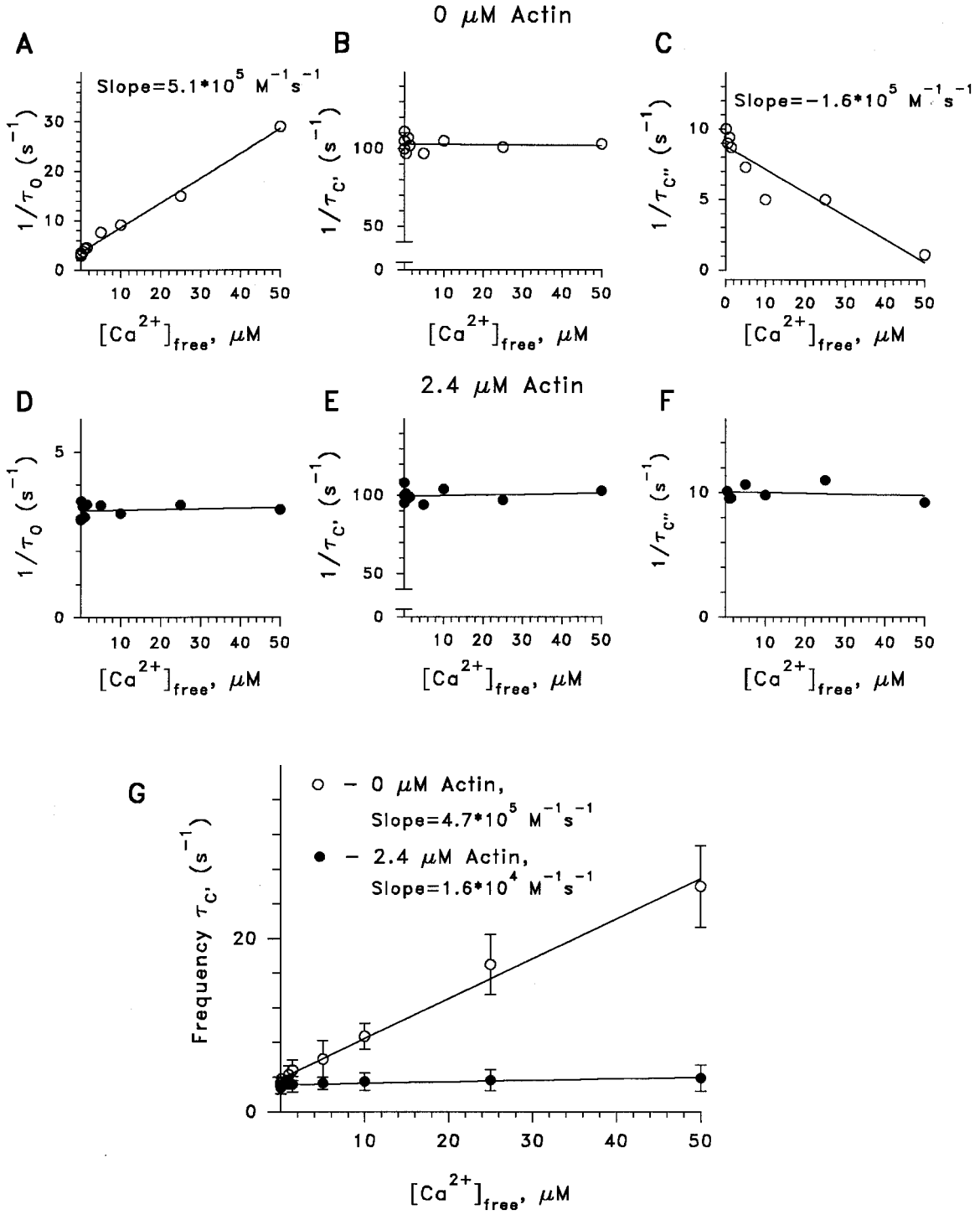

FIGURE 5 Analyses of the times spent by α-ENaC in open and closed states versus $[Ca^{2+}]$. Data points represent the reciprocals of the dwell time constants of ENaC in the (*A—C*) absence, and (*D—F*) presence of actin determined as described in Fig. 4. Numbers next to the plots represent the slopes of the first-order regression fits of the data (if different from zero). (*G*) The frequency of appearance of the short-lived closed state per unit open time was calculated as the total number of events spent by the channel in the short-lived closed state (the sum of the probability density function fitting the short lived component of the closed time histogram, see dotted lines in the histograms in Fig. 4), normalized for the time spent by the channel in the open state (the integral of the probability density function fitting the open time histogram). Numbers next to the plots represent the slopes of the first-order regression fits of the data.

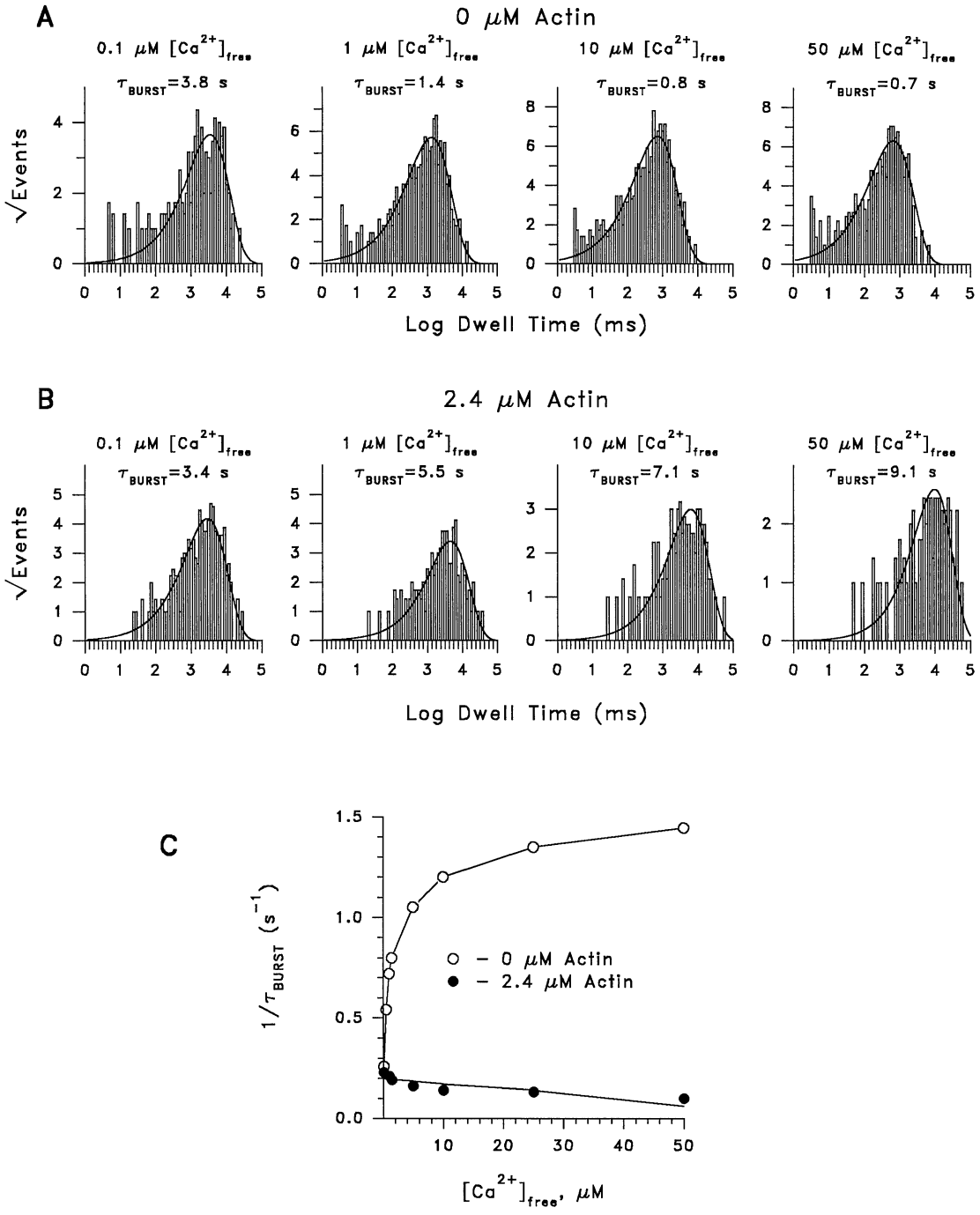

FIGURE 6 Effect of $[Ca^{2+}]$ on duration of bursts of α-rENaC activity in the absence and in the presence of actin. Burst dwell time histograms were built from the events lists constructed by the pCLAMP software (Axon Instruments) for single-channel recordings of 20 min in length acquired as described in Fig. 1. The bursts were recognized by setting the closed-time duration threshold at one-third of the mean dwell time spent by the channel in the second closed state (defined as a Ca^{2+}-blocked state), and the 50% amplitude crossing threshold. Burst-time constants shown were determined by fitting the data to the probability density function (Eq. 10) using the simplex least square routine of pSTAT. Numbers of events used for construction of the histograms shown in (*A*) (in the absence of the actin) were: 255 (0.1 μM Ca^{2+}), 614 (1 μM Ca^{2+}), 799 (10 μM Ca^{2+}), and 752 (100 μM Ca^{2+}). Histograms shown in (*B*) (in the presence of the actin) were constructed from 328 (0.1 μM Ca^{2+}); 207 (1 μM Ca^{2+}), 160 (10 μM Ca^{2+}), and 110 (50 μM Ca^{2+}) events. Number of bins per decade in all histograms was 16. (*C*) Lines in the graph represent the second- and the first-order regression fits of the reciprocal burst time constants determined as shown in (*A*) and (*B*), respectively.

TABLE 2 Effect of actin on duration of α-ENaC activity delimited by $[Ca^{2+}]_{free}$-induced long-lived closures

$[Ca^{2+}]_{free}$ (μM)	τ_{burst} (M ± m, s)		Minimum number of events fitted in a single experiment		Number of experiments	
	0 μM Actin	2.4 μM Actin	0 μM Actin	2.4 μM Actin	0 μM Actin	2.4 μM Actin
0.100	3.85 ± 0.63	4.34 ± 1.23	234	303	5	5
0.491	1.85 ± 0.51	4.41 ± 1.69	493	257	4	3
0.983	1.39 ± 0.44	4.76 ± 1.38	591	188	5	4
1.440	1.25 ± 0.35	5.26 ± 1.24	609	212	3	4
5.000	0.95 ± 0.37	6.25 ± 1.65	647	184	3	3
10.00	0.83 ± 0.27	7.14 ± 1.44	753	149	4	4
25.0	0.74 ± 0.24	7.69 ± 2.32	682	122	4	3
50.0	0.69 ± 0.22	10.04 ± 3.17	704	96	4	4

single-channel kinetics are consistent with the idea that, in the presence of actin, Ca^{2+} acts as a fast-to-intermediate open channel blocker of ENaC.

This work was supported by National Institutes of Health Grants DK37206 and DK56095 (D.J.B.), and the grants FONDECYT 100-0890 (R.L.) and Cátedra Presidencial, a Human Frontier in Science Program grant (R.L.), and by a group of Chilean companies (AFP Protection, CODELCO, Empresas CMPC, CGE, Gener S.A., Minera Escondida, Minera Collahuasi, NOVAGAS, Business Design Assoc., and XEROX Chile) (R.L.). The Centro de Estudios Cientificos is a Millenium Science Institute.

I.I.I. is a recipient of the Lazaro J. Mandel Memorial Award from the American Physiological Society.

REFERENCES

Awayda, M. S., I. I. Ismailov, B. K. Berdiev, and D. J. Benos. 1995. A cloned renal epithelial Na^+ channel protein displays stretch activation in planar lipid bilayers. *Am. J. Physiol. Cell Physiol.* 268:C1450–C1459.

Berdiev, B. K., K. H. Karlson, B. Jovov, P. J. Ripoll, R. Morris, D. Loffing-Cueni, P. Halpin, B. A. Stanton, T. R. Kleyman, and I. I. Ismailov. 1998. Subunit stoichiometry of a core conduction element in a cloned epithelial amiloride-sensitive Na^+ channel. *Biophys. J.* 75: 2292–2301.

Berdiev, B. K., A. G. Prat, H. F. Cantiello, D. A. Ausiello, C. M. Fuller, B. Jovov, D. J. Benos, and I. I. Ismailov. 1996. Regulation of epithelial sodium channels by short actin filaments. *J. Biol. Chem.* 271: 17704–17710.

Bers, D. M. 1982. A simple method for the accurate determination of free [Ca] in Ca-EGTA solutions. *Am. J. Physiol. Cell Physiol.* 242: C404–C408.

Brooks, S. P., and K. B. Storey. 1992. Bound and determined: a computer program for making buffers of defined ion concentrations. *Anal. Biochem.* 201:119–126.

Canessa, C. M., J.-D. Horisberger, and B. C. Rossier. 1993. Epithelial sodium channel related to proteins involved in neurodegeneration. *Nature.* 361:467–470.

Canessa, C. M., L. Schild, G. Buell, B. Thoreus, I. Gautschi, J.-D. Horisberger, and B. C. Rossier. 1994. Amiloride-sensitive epithelial Na^+ channel is made of three homologous subunits. *Nature.* 367:463–467.

Cantiello, H. F. 1995. Role of the actin cytoskeleton on epithelial Na^+ channel regulation. *Kidney Int.* 48:970–984.

Cantiello, H. F. 1997a. Changes in actin filament organization regulate Na^+,K^+-ATPase activity. Role of actin phosphorylation. *Ann. N.Y. Acad. Sci.* 834:559–561.

Cantiello, H. F. 1997b. Role of actin filament organization in cell volume and ion channel regulation. *J. Exp. Zool.* 279:425–435.

Cantiello, H. F., and A. G. Prat. 1996. Role of actin filament organization in ion channel activity and cell volume regulation. *In* Membrane Protein-Cytoskeleton Interactions. Current Topics in Membranes. W. J. Nelson, editor. Academic Press, San Diego. 373–396.

Cantiello, H. F., J. L. Stow, A. G. Prat, and D. A. Ausiello. 1991. Actin filaments regulate epithelial Na^+ channel activity. *Am. J. Physiol. Cell Physiol.* 261:C882–C888.

Carlier, M. F. 1990. Actin polymerization and ATP hydrolysis. *Adv. Biophys.* 26:51–73.

Carlier, M. F., D. Pantaloni, J. A. Evans, P. K. Lambooy, E. D. Korn, and M. R. Webb. 1988. The hydrolysis of ATP that accompanies actin polymerization is essentially irreversible. *FEBS Lett.* 235:211–214.

Carlier, M. F., D. Pantaloni, and E. D. Korn. 1986a. Fluorescence measurements of the binding of cations to high-affinity and low-affinity sites on ATP-G-actin. *J. Biol. Chem.* 261:10778–10784.

Carlier, M. F., D. Pantaloni, and E. D. Korn. 1986b. The effects of Mg^{2+} at the high-affinity and low-affinity sites on the polymerization of actin and associated ATP hydrolysis. *J. Biol. Chem.* 261:10785–10792.

Carlier, M. F., D. Pantaloni, and E. D. Korn. 1987. The mechanisms of ATP hydrolysis accompanying the polymerization of Mg-actin and Ca-actin. *J. Biol. Chem.* 262:3052–3059.

Cooper, J. A., E. L. Buhle, Jr., S. B. Walker, T. Y. Tsong, and T. D. Pollard. 1983. Kinetic evidence for a monomer activation step in actin polymerization. *Biochemistry.* 22:2193–2202.

Cowin, P., and B. Burke. 1996. Cytoskeleton-membrane interactions. *Curr. Opin. Cell Biol.* 8:56–65.

Estes, J. E., L. A. Selden, H. J. Kinosian, and L. C. Gershman. 1992. Tightly-bound divalent cation of actin. *J. Muscle Res. Cell Motil.* 13: 272–284.

Fabiato, A., and F. Fabiato. 1979. Calculator programs for computing the composition of the solutions containing multiple metals and ligands used for experiments in skinned muscle cells. *J. Physiol. (Paris).* 75:463–505.

Fuchs, E., and Y. Yang. 1999. Crossroads on cytoskeletal highways. *Cell.* 98:547–550.

Green, W. N., L. B. Weiss, and O. S. Andersen. 1987. Batrachotoxin-modified sodium channels in planar lipid bilayers. Ion permeation and block. *J. Gen. Physiol.* 89:841–872.

Harrison, S. M., and D. M. Bers. 1989. Correction of absolute stability constants of EGTA for temperature and ionic strength. *Am. J. Physiol. Cell Physiol.* 256:C1250–C1256.

Hilgemann, D. W. 1997. Cytoplasmic ATP-dependent regulation of ion transporters and channels: mechanisms and messengers. *Annu. Rev. Physiol.* 59:193–220.

Hitchcock, S. E. 1980. Actin deoxyrobonuclease I interaction. Depolymerization and nucleotide exchange. *J. Biol. Chem.* 255:5668–5673.

Hitchcock, S. E., L. Carisson, and U. Lindberg. 1976. Depolymerization of F-actin by deoxyribonuclease I. *Cell.* 7:531–542.

Hu, S., and L. F. Reichardt. 1999. From membrane to cytoskeleton: enabling a connection. *Neuron.* 22:419–422.

Ismailov, I. I., M. S. Awayda, B. K. Berdiev, J. K. Bubien, J. E. Lucas, C. M. Fuller, and D. J. Benos. 1996. Triple-barrel organization of ENaC, a cloned epithelial Na^+ channel. *J. Biol. Chem.* 271:807–816.

Ismailov, I. I., B. K. Berdiev, V. Gh. Shlyonsky, C. M. Fuller, A. G. Prat, B. Jovov, H. F. Cantiello, D. A. Ausiello, and D. J. Benos. 1997a. Role of actin in regulation of epithelial sodium channels by CFTR. *Am. J. Physiol. Cell Physiol.* 272:C1077–C1086.

Ismailov, I. I., V. Gh. Shlyonsky, O. Alvarez, and D. J. Benos. 1997b. Cation permeability of a cloned rat epithelial amiloride-sensitive Na^+ channel. *J. Physiol.* 504:287–300.

Ismailov, I. I., V. Gh. Shlyonsky, E. H. Serpersu, C. M. Fuller, H. C. Cheung, D. Muccio, B. K. Berdiev, and D. J. Benos. 1999. Peptide inhibition of ENaC. *Biochemistry.* 38:354–363.

Janmey, P. A. 1998. The cytoskeleton and cell signaling: component localization and mechanical coupling. *Physiol. Rev.* 78:763–781.

Kabsch, W., and J. Vandekerckhove. 1992. Structure and function of actin. *Annu. Rev. Biophys. Biomol. Struct.* 21:49–76.

Kinosian, H. J., L. A. Selden, J. E. Estes, and L. C. Gershman. 1991. Thermodynamics of actin polymerization: influence of the tightly bound divalent cation and nucleotide. *Biochim. Biophys. Acta.* 1077:151–158.

Korn, E. D., M. F. Carlier, and D. Pantaloni. 1987. Actin polymerization and ATP hydrolysis. *Science.* 238:638–644.

Lingueglia, E., N. Voilley, R. Waldmann, M. Lazdunski, and P. Barbry. 1993. Expression cloning of an epithelial amiloride-sensitive Na^+ channel. A new channel type with homologies to *Caenorhabditis elegans* degenerins. *FEBS Lett.* 318:95–99.

Mannherz, H. G., J. B. Leigh, R. Leberman, and H. Pfrang. 1975. A specific 1:1 G-actin:DNAase I complex formed by the action of DNAase I on F-actin. *FEBS Lett.* 60:34–38.

Mills, J. W., and L. J. Mandel. 1994. Cytoskeletal regulation of membrane transport events. *FASEB J.* 8:1161–1165.

Pollard, T. D., and J. A. Cooper. 1986. Actin and actin-binding proteins. A critical evaluation of mechanisms and functions. *Ann. Rev. Biochem.* 55:987–1035.

Pollard, T. D., and A. G. Weeds. 1984. The rate constant for ATP hydrolysis by polymerized actin. *FEBS Lett.* 170:94–98.

Prat, A. G., A. M. Bertorello, D. A. Ausiello, and H. F. Cantiello. 1993. Activation of epithelial Na^+ channels by protein kinase A requires actin filaments. *Am. J. Physiol. Cell Physiol.* 265:C224–C233.

Sheng, M., and D. T. S. Pak. 2000. Ligand-gated ion channel interactions with cytoskeletal and signaling proteins. *Annu. Rev. Physiol.* 62: 755–778.

Sigworth, F. J., and S. M. Sine. 1987. Data transformations for improved display and fitting of single-channel dwell time histograms. *Biophys. J.* 52:1047–1054.

Smith, G. L., and D. J. Miller. 1985. Potentiometric measurements of stoichiometric and apparent affinity constants of EGTA for protons and divalent ions including calcium. *Biochim. Biophys. Acta.* 839:287–299.

Smith, P. R., and D. J. Benos. 1996. Regulation of epithelial ion channel activity by the membrane-cytoskeleton. *In* Membrane Protein-Cytoskeleton Interactions. Current Topics in Membranes. W. J. Nelson, editor. Academic Press, San Diego. 345–372.

Smith, P. R., G. Saccomani, E. H. Joe, K. J. Angelides, and D. J. Benos. 1991. Amiloride-sensitive sodium channel is linked to the cytoskeleton in renal epithelial cells. *Proc. Natl. Acad. Sci. U.S.A.* 88:6971–6975.

Staub, O., S. Dho, P. Henry, J. Correa, T. Ishikawa, J. McGlade, and D. Rotin. 1996. WW domains of Nedd4 bind to the proline-rich PY motifs in the epithelial Na^+ channel deleted in Liddle's syndrome. *EMBO J.* 15:2371–2380.

Tsien, R. Y. 1980. New calcium indicators and buffers with high selectivity against magnesium and protons: design, synthesis, and properties of prototype structures. *Biochemistry.* 19:2396–2404.

Vergara, C., and R. Latorre. 1983. Kinetics of Ca^{2+}-activated K^+ channels from rabbit muscle incorporated into planar bilayers. Evidence for a Ca^{2+} and Ba^{2+} blockade. *J. Gen. Physiol.* 82:543–568.

Villarroel, A., O. Alvarez, A. Oberhauser, and R. Latorre. 1988. Probing a Ca^{2+}-activated K^+ channel with quaternary ammonium ions. *Pflug. Arch.* 413:118–126.

Wang, G. K. 1988. Cocaine-induced closures of single batrachotoxin-activated Na^+ channels in planar lipid bilayers. *J. Gen. Physiol.* 92: 747–765.

Yellen, G. 1984. Ionic permeation and blockade in Ca^{2+}-activated K^+ channels of bovine chromaffin cells. *J. Gen. Physiol.* 84:157–186.

Zigmond, S. H. 1996. Signal transduction and actin filament organization. *Curr. Opin. Cell Biol.* 8:66–73.